NANO · MICRO small
www.small-journal.com

Self-Assembly of DNA Origami Heterodimers in High Yields and Analysis of the Involved Mechanisms

*Breveruos Sheheade, Miran Liber, Mary Popov, Yaron Berger, Dinesh C. Khara, Jürgen Jopp, and Eyal Nir**

Efficient fabrication of structurally and functionally diverse nanomolecular devices and machines by organizing separately prepared DNA origami building blocks into a larger structure is limited by origami attachment yields. A general method that enables attachment of origami building blocks using 'sticky ends' at very high yields is demonstrated. Two different rectangular origami monomers are purified using agarose gel electrophoresis conducted in solute containing 100×10^{-3} M NaCl, a treatment that facilitates the dissociation of most of the incorrectly hybridized origami structures that form through blunt-end interactions during the thermal annealing process and removes these structures as well as excess strands that otherwise interfere with the desired heterodimerization reaction. Heterodimerization yields of gel-purified monomers are between 98.6% and 99.6%, considerably higher than that of monomers purified using the polyethylene glycol (PEG) method (88.7–96.7%). Depending on the number of PEG purification rounds, these results correspond to about 4- to 25-fold reduction in the number of incorrect structures observed by atomic force microscopy. Furthermore, the analyses of the incorrect structures observed before and after the heterodimerization reactions and comparison of the purification methods provide valuable information on the reaction mechanisms that interfere with heterodimerization.

1. Introduction

The DNA origami technique has been demonstrated to be effective for rational and programmable organization of diverse molecular species with near atomic precision.[1–6] DNA origami constructs have been used to organize metallic nanostructures,[7–12] proteins and enzymes,[13–16] carbon nanotubes,[17,18] and organic polymers[19] and as structural scaffolds for dynamic molecular devices and machines such as a molecular assembly line,[20] molecular motors,[21–25] force clamp devices,[26,27] a nanorobot for drug delivery,[28] a molecular sorting robot,[29] and DNA nanochip for base-excision repair.[30] The size, architectural diversity, and chemical addressability of these molecular constructs were limited, however, as all were fabricated from a single origami unit.[31] To overcome size limitations, identical origami units have been polymerized into linear and other 2D structures, and structures composed of hundreds of units have been achieved.[32–38] However, with this approach, the origami monomers are typically free to polymerize uncontrollably. In addition, because the monomers are typically identical, addressability and diversity remain limited.

In principle, structures with almost any desired architecture and size could be created using a Lego-like approach in which diverse origami building blocks, each designed with unique connectivity and prepared and pre-functionalized separately, are joined together.[1,39–54] With few exceptions,[54] origami attachment has been achieved by hybridization of 'sticky ends',[1,39–44] by blunt-end stacking interactions of helices,[45–48] or by the combination of the two methods.[49–53] With these methods, origami addressability and reaction hierarchy is typically achieved by the sticky ends sequences and the locations of the blunt ends and can be further assisted by use of complementary origami shapes.[45,49–51]

In practice, however, the assembly efficiencies of structures fabricated from different origami units are typically not particularly high. For example, using the sticky-ends method, dimers were assembled in yields ranging from 80% to 90%[40–42] and octamers yields were only 63%.[43] These represent 80%[40] to 95%[43] attachment reaction yields for every origami monomer added to the structure. Using only or predominately stacking interactions, tetramer (44% total yield[45]), pentamers (24%,[50] 31%,[45] and 74%[48]), octamer (46%[48]), and nonamers (35%[51] and 41%[48]) were fabricated with 70%[50] to 92%[48] yields for every added monomer. In a recent notable study, Tikhomirov et al. constructed 2×2, 4×4, and 8×8 origami arrays made of 4, 16, and 64 unique origami tiles using stacking interactions

B. Sheheade, Dr. M. Liber, Dr. M. Popov, Dr. Y. Berger, Dr. D. C. Khara, Dr. J. Jopp, Prof. E. Nir
Department of Chemistry and the Ilse Katz Institute for Nanoscale Science and Technology
Ben-Gurion University of the Negev
Beer Sheva 84105, Israel
E-mail: eyalnir@bgu.ac.il

The ORCID identification number(s) for the author(s) of this article can be found under https://doi.org/10.1002/smll.201902979.

DOI: 10.1002/smll.201902979

and short sticky ends (of 1 or 2 nucleotides in length) and hierarchical assembly at total yields of 93%, 48%, and 1.8%, respectively.[53] The attachment yields of each additional tile decreased only slightly with the increase in the number of tiles (from 97.6% to 93.8%),[53] and the authors of this work suggest that the weak stacking interactions allowed rearrangements that helped building blocks escape kinetic traps during assembly in the complex reaction mixture environment.

It is clear that increased number of building blocks with different addressabilities increases the complexity of the origami assembly reaction, and thus, lowers the total yield.[6,53] It is unclear, however, why the total yields of structures that consist of only a small number of origami units are typically not high. The dynamics of sticky end-based origami attachment reactions have been studied,[39,40,55] but the reasons for the low yields remain unknown. Using single-molecule fluorescence to study heterodimerization and heterodimer dissociation kinetics, we recently showed that the low yields of sticky end-based heterodimerization (typically 85–90%) cannot be explained by thermodynamic instability or by structural imperfections of the origami constructs.[42] We hypothesized that the low heterodimerization yields are due to preformation of stable homodimers that hinder the formation of the correct heterodimers and speculated that removing these unwanted structures would increase heterodimerization yields, and this hypothesis was examined here.

The goals of this study were to develop a method for dimerization of two different origami units with high yields using the addressable sticky-ends method and to understand the factors that hinder heterodimerization. By atomic force microscopy (AFM), we observed that origami structures consisting of 'bridging strands' (edge staples that contain the sticky ends) form homodimers and larger structures through blunt-end interactions. Analysis before sample purification, after agarose gel electrophoresis (gel) purification or after polyethylene glycol (PEG) purification,[56,57] and analysis after the heterodimerization reaction revealed a rather complex picture. Homodimers and larger structures were extensively formed in the thermal annealing process. Purification of the origami samples using gel containing 100×10^{-3} M NaCl facilitated the dissociation of these structures into their monomeric forms and removed structures that did not dissociate as well as removing excess strands. The PEG purification method did not remove these unwanted structures. Extraction of monomers from the gel and reaction with the corresponding monomers resulted in heterodimerization yields considerably higher than that of monomers purified using the PEG method. Homodimers were reformed through the interactions of origami bridging-strand edges (BSEs) after the annealing process (and after gel purification), but these homodimers dissociated in the presence of the other origami type and thus did not substantially interfere with the heterodimerization reaction. Homodimers formed through the interaction of BSEs with poly-thymine (poly-T) loop edges in the thermal annealing process were not observed after gel purification. These homodimers were not removed by the PEG purification method, and, therefore, reduced heterodimer yields. In addition, we showed that removal of excess strands was essential for achieving high heterodimerization yields.

2. Results

2.1. Origami Monomer Design and the Sticky-End Attachment Technique

The origami monomers were based on the Rothemund rectangle origami[1] with minor modifications and were assembled by temperature-gradient annealing as previously described.[42] For detailed origami monomer design and preparation procedures and scaffold and strand sequences see the Experimental Section and Supporting Information. To enable recognition of the monomer type and orientation, the two monomers were imprinted with the letters 'F' and 'G' using the 'dumbbell staple' technique.[1] To enable formation of heterodimers, the right-side edge of origami-F and the left-side edge of origami-G monomers were prepared with bridging strands consisting of complementary sticky-end sequences (**Figure 1**a,b). Origami monomers had 7 or 12 bridging strands that, upon origami heterodimerization, formed 11 or 23 sticky-end connections (Figures 1b,c, respectively). The lengths of the sticky ends were 5, 8, or 11 nucleotides. The left-hand side of origami-F and right-hand side of origami-G were prepared with 12 scaffold-complementary strands containing poly-T loops (Figures 1a,d).[1,42] The origami nomenclatures are as follows: Fx/y and Gx/y refer to origami-F or origami-G monomers, respectively, with x equal to the number of sticky ends of length y, and FGx/y refer to the corresponding heterodimer. Origami-F0 and origami-G0 refer to monomers without bridging strands on one edge (but with poly T-loop strands on the other edge).

2.2. Monomer Self-Interactions and High Heterodimerization Yields Achieved Using Gel Purification

The significant formation of homodimers and larger structures via BSE interactions in the thermal annealing process is evident in AFM images of unpurified origami samples. There were almost no homodimers in the origami F0 and G0 samples, whereas samples of origamis F23/8 and G23/8 showed significant formation of homodimers and, to a lesser extent, homotrimers (**Figure 2**a, 40% and 43% F23/8 and G23/8 homodimers, respectively, and Figure S1, Supporting Information). The effect of the origami edge design on the formation of homodimers and larger structures was further analyzed by agarose gel electrophoresis performed with a solute containing 12×10^{-3} M $MgCl_2$. The analysis showed that origami monomers with edges containing the full set of bridging strands formed significantly more homodimers and larger structures than did those without bridging strands (F23 and G23 versus F0 and G0, Figure 2b), in agreement with the AFM data. Moreover, for the same sticky-end lengths, a decrease in the number of bridging strands decreased the formation of homodimers and larger structures. Importantly, for the same number of bridging strands, longer sticky ends also decreased the formation of homodimers and larger structures. As is explained in detail below, longer sticky ends reduce the formation of blunt-end interactions between the origami edges and, as a result, the formation of homodimers.

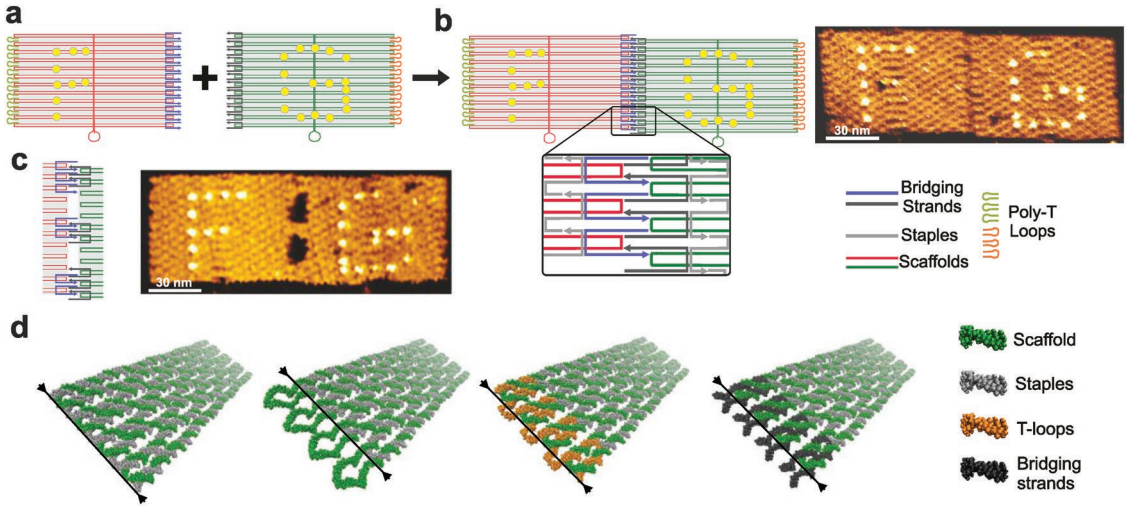

Figure 1. Origami design and sticky-end heterodimerization technique. a) Schematics of origami-F and origami-G monomers (F23/8 and G23/8, respectively). Each of these monomers consists of 12 bridging strands (shown in blue and dark gray), 12 poly-T loop strands (shown in cyan and orange), and a scaffold (shown in red and green). Staples are shown in light gray, and yellow circles represent the locations of the 'F' and 'G' dumbbell staples. b) Schematics of the FG23/8 heterodimer formed via hybridization of the 23 sticky ends and a corresponding AFM image. c) Schematic of the attachment site of FG11/8 heterodimer and a corresponding AFM image. d) Schematics of different origami edge designs. From left to right are origami functionalized with edge staples, origami without edge staples (shown in green are the scaffold loops), origami with poly-T loop strands, and origami with bridging strands. The arrows indicate the locations of the blunt ends of the helices.

Magnesium ions carry two positive charges and are effective in neutralizing DNA negative charge. As such, these ions reduce ionic repulsion forces between DNA molecules,[58] making non-specific DNA interactions more likely. Realizing that in some cases monomers bands were almost completely absent and therefore could not be extracted from gels loaded

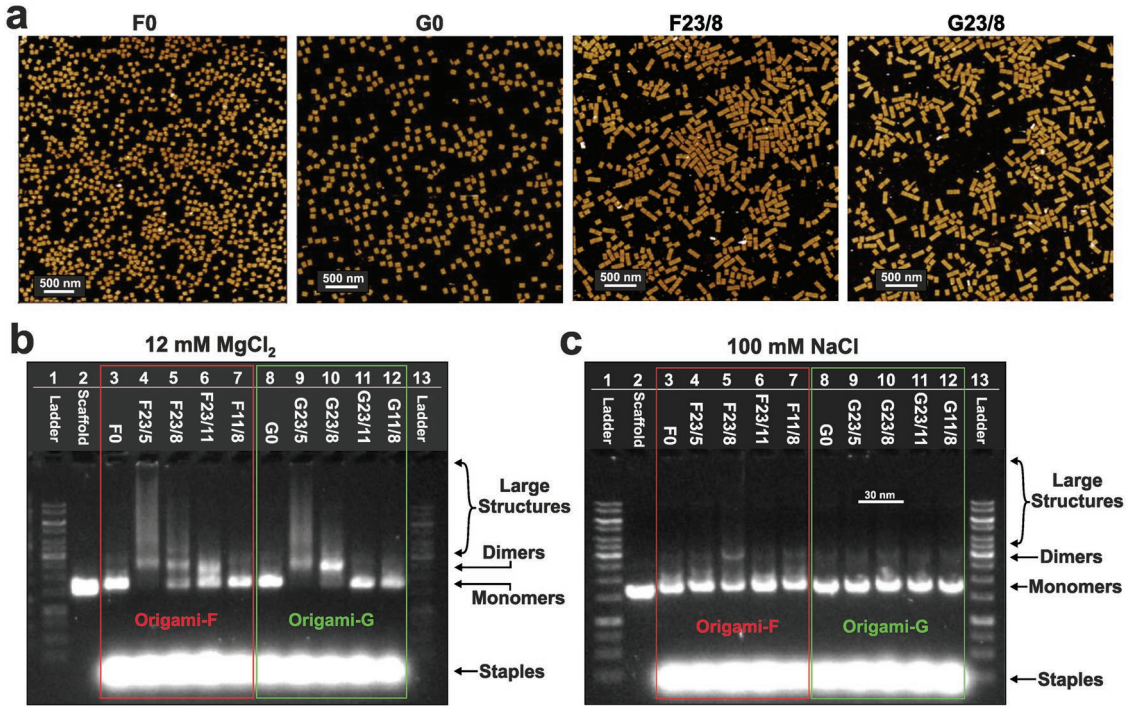

Figure 2. Evidence for the formation of homodimers and larger structures in the thermal annealing process and of the ability to dissociate these structures to their monomeric form using agarose gels containing NaCl. a) AFM images of unpurified F0, G0, F23/8, and G23/8. b) Agarose gel chromatogram analysis (conducted in a solution containing 12×10^{-3} M $MgCl_2$) of origami-F and origami-G without bridging strands (Lanes 3 and 8, respectively), with 12 bridging strands (23 sticky ends) of the lengths 5, 8, and 11 nt (Lanes 4–6 and 9–11, respectively), and with 7 bridging strands (11 sticky ends) of the length 8 nt (Lanes 7 and 12, respectively). Lanes 1 and 13 were loaded with 1-kb ladder and lane 2 with M13mp18 scaffold. c) Agarose gel chromatogram in a solution containing 100×10^{-3} M NaCl. Lanes are the same as for panel b).

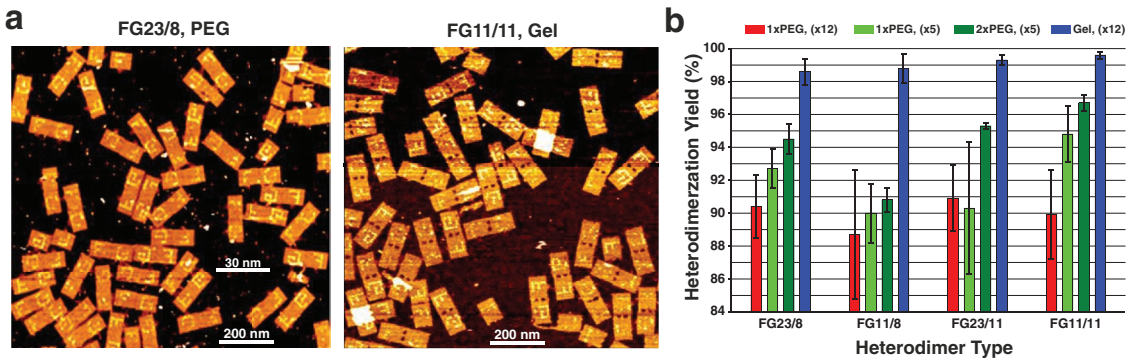

Figure 3. Heterodimerization yields. a) Representative AFM images of FG23/8 and FG11/11 heterodimers prepared using the PEG and the agarose gel purification methods. For additional AFM images, see Figures S3–S7 in the Supporting Information. b) Summary of heterodimerization yields of monomers prepared with × 12 or × 5 excess poly-T loops and bridging strands and purified once or twice using PEG (1 × PEG(× 12), 1 × PEG(× 5), and 2 × PEG(× 5), respectively) and of monomers purified using the agarose gel method. Monomers were functionalized with 23 or 11 sticky ends of lengths 8 or 11 nts. Heterodimerization yields were calculated according to a method described in the Experimental Section.

with Mg^{2+}-containing solution, we used a gel prepared and run in buffer with singly charged sodium ions (100×10^{-3} M NaCl) as a means to enhance dissociation of the homodimers and larger structures into their monomeric components. Under conditions with only monovalent ions, we observed almost complete dissociation of the non-specific structures into their monomeric components (Figure 2c). Dissociation of homodimers and larger structures was also achieved using buffer with 4×10^{-3} M $MgCl_2$ (Figure S2, Supporting Information). However, the results were more consistent with buffer containing 100×10^{-3} M NaCl than with the 4×10^{-3} M $MgCl_2$ buffer, and therefore NaCl buffer was used for the rest of this study.

Monomers were extracted from the agarose gels, and samples were concentrated using PEG precipitation (see the Experimental Section). Origami-F monomers and the corresponding origami-G monomers were mixed at room temperature (reaction mixture), incubated for 48 h, and the heterodimerization yields of FG23/8, FG11/8, FG23/11, and FG11/11 were determined using AFM. In addition, we also determined the heterodimerization yields of these four pairs of monomers purified by the PEG method. Representative AFM images are shown in **Figure 3**a; additional images are shown in Figures S3–S7 in the Supporting Information. To study the influence of unpurified poly-T loop and bridging strands on the heterodimerization reaction yields, samples that were purified by the PEG method were annealed either with the same ratio of poly-T loop and bridging strands to scaffold concentrations as the monomers purified by gel (x 12) or were prepared with reduced strand to scaffold ratios (x 5), and the monomer samples were either PEG purified once or twice. In all cases, the heterodimerization yields were higher for the gel-purified samples (maximum of 99.6% yield for FG11/11) than for the PEG-purified samples (maximum of 96.7% yield for FG11/11, Figure 3b). These correspond to 4- to 25-fold decrease in incorrect structures for the gel purified samples in comparison to PEG purified samples. Furthermore, for the PEG-purified samples, heterodimerization yields generally increased with the decrease of unpurified poly-T loops and bridging strands (Figure 3b, red, light green, and dark green columns, respectively).

2.3. Characterization of the Homodimers and Homotrimers

To understand the factors that support or prevent correct heterodimerization, we characterized the homodimers and homotrimers observed after PEG and gel purification. Analysis of the AFM images of PEG purified origami-F and origami-G samples (in the absence of the other origami type) show that about 46% of origami-F and 49% of origami-G formed homodimers (and some homotrimers Figures S8 and S9, Supporting Information). Classification of the origami interactions showed that most (86% for origami-F and 93% for origami-G) were between the BSEs either in the 'flip' or the 'rotate' orientations (**Figure 4**, 'BSE–BSE'). In addition, and important for our analysis, interactions were also formed between the origami BSE and the poly-T edge (Figure 4, 'BSE–PTE', 14% for origami-F and 7% for origami-G). Homodimers and homotrimers formed through PTE–PTE interaction or through BSE–BSE or BSE–PTE in other orientations were only rarely observed (<0.2% of the structures).

To study whether such structures can also be formed after the annealing process, we purified origami-F and origami-G using an agarose gel (100×10^{-3} M NaCl), incubated the extracted monomers in 12×10^{-3} M $MgCl_2$ for 24 h, and characterized the samples using AFM. The results show that 40% of origami-F and 44% of origami-G monomers formed homodimers (and some homotrimers, Figures S10 and S11, Supporting Information). Almost all the homodimers were formed through BSE–BSE interactions (99% for origami-F and 98% for origami-G, respectively, Figure 4), and only about 1% were formed through BSE–PTE interactions.

2.4. Characterization of Incorrect Structures Present in Reaction Mixtures

Analysis of the AFM images of origami-F/origami-G reaction mixtures show that monomers constitute the majority of the incorrect structures observed at the end of the reaction for most of the PEG-purified samples and were almost the only incorrect structures for the gel-purified samples (**Figure 5**a,

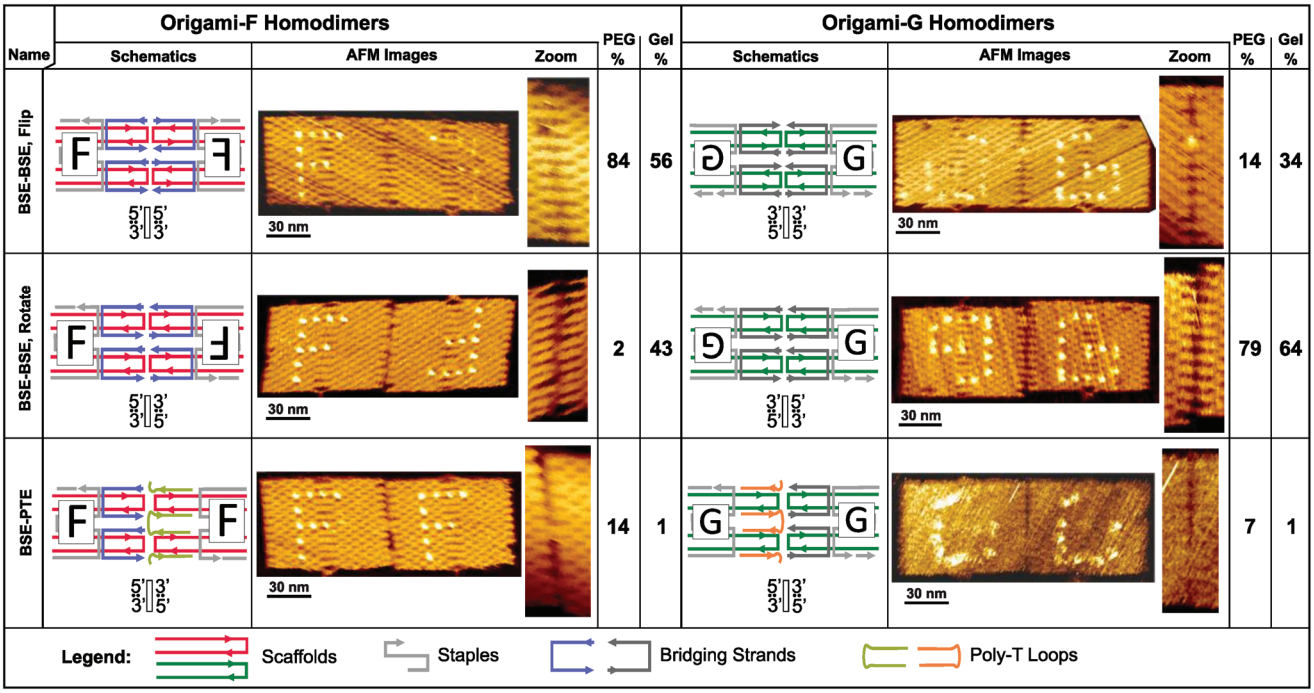

Figure 4. Types of homodimers formed by origami-F (left) and origami-G (right). Schematics, AFM images, and relative frequencies of different homodimer constructs are shown. Homodimers are formed through interactions of BSEs in a flip and rotate orientations (BSE–BSE flip and BSE–BSE rotate, upper and middle rows, respectively) and through interactions between BSE–PTE (lower row). Scaffolds, poly-T loops, and bridging strands are marked with arrows to indicate strand directionalities (5′→3′). The numbers are the percentages of the corresponding homodimers observed after PEG and gel purifications (left- and right-hand columns, respectively).

light green columns). The second most common incorrect structure, observed almost exclusively in the PEG-purified samples, were heterotrimers of the form FFG and FGG (Figure 5a, red columns; Figure 5b). Analysis of the structures of the heterotrimers showed that the FG heterodimers in these heterotrimers structures were connected through the designated bridging strands and were in the correct orientation. The additional origami-F or origami-G was connected to origami-F or origami-G of the FG heterodimer, respectively, as in the BSE–PTE interaction shown in Figure 4. Other incorrect structures, such as homodimers, incorrect heterodimers, and trimers other than FFG and FGG constituted at most 1% of the total structures (Figure 5, part of the contribution to the blue columns). These results mean that origami-F and origami-G interact with each other almost exclusively through the designated bridging strands and in the correct orientation. Cases in which origami-F and origami-G monomers interacted with each other incorrectly (e.g., in a BSE–PTE fashion) constituted at most 0.2% of the total structures (Figure 5a, part of the contribution to the blue columns). Surprisingly, BSE–BSE interactions between identical monomers, which was the interaction observed in the majority of the homodimers (Figure 4), were rarely observed in the reaction mixtures (0%–0.1%, depending on the sample). This means that in the presence of the other origami type, the BSE–BSE homodimers (whether formed during or after the annealing process) dissociate almost completely and the monomers associate to form the desired heterodimers.

3. Discussion

3.1. Mechanisms that Influence Heterodimerization Reaction Yields and Importance of Monomer Purification

Effective fabrication of origami-based nanomolecular devices from separately prepared DNA origami building blocks requires high yields of building block attachment. Here, we demonstrated that the yield of heterodimerization of origami building blocks with sticky ends was increased relative to the standard PEG purification method when origami monomers were purified using agarose gel electrophoresis. We also identified factors that support and prevent correct heterodimerization. It is important to note the differences between the gel and the PEG purification methods. The gel method separates the origami monomers species from the free DNA strands (i.e., bridging strands, poly-T loop strands, and staples) and from the origami dimers and larger species to allow near complete purification of the monomer samples (Figure 2b,c). In contrast, PEG purification does not entirely remove excess strands from the monomer solution, and the method is incapable of separating dimers and larger structures from monomer structures (as was shown using gel, Figure S2, Supporting Information, and AFM, Figure 4). These two advantages resulted in higher heterodimerization yields for gel purified samples over PEG purified samples for each of the four different origami bridging-strand designs studied here (Figure 3c). Origami monomers and FFG and FGG heterotrimers constituted the main

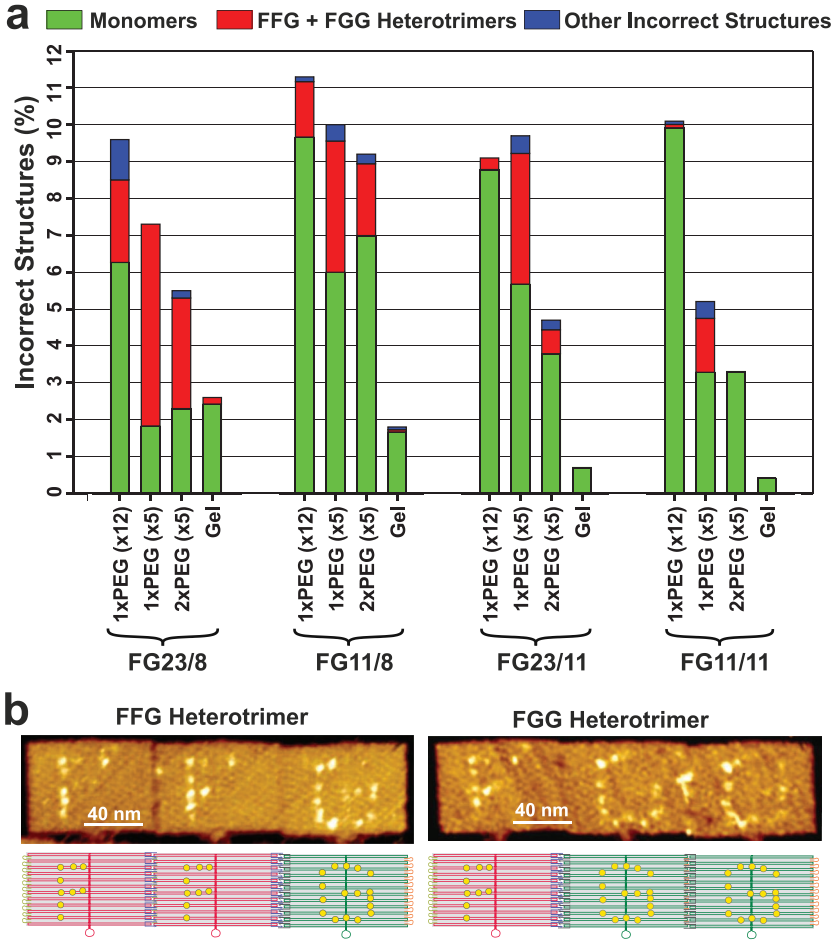

Figure 5. Incorrect structures observed in the heterodimerization reaction mixtures. a) Summary of the fractions of incorrect structures observed using AFM in mixtures of monomers purified using PEG (1 × PEG(× 12), 1 × PEG(× 5), 2 × PEG(× 5)), and agarose gel electrophoresis. Percentages of monomers, FFG and FGG heterotrimers, and other incorrect structures are indicated by green, red, and blue, respectively. b) AFM images and schematics of FFG and FGG heterotrimers.

incorrect structures observed after the heterodimerization reaction (Figure 5). These species influence the heterodimerization yields, and therefore the mechanisms that explain the presence of monomers and the formation of the FFG and FGG heterotrimers are of interest.

Unreactive Monomers: In most cases, the percentage of residual monomers decreased with the decrease in the level of poly-T loops and bridging strands present in the heterodimerization reaction solution as shown by analysis of heterodimerization of monomers purified once or twice by PEG precipitation and of monomers purified by gel (Figure 3c). These results indicate that residual strands interfere with the heterodimerization reaction. We suggest that unpurified bridging strands belonging to the hypothetical origami-X hybridize via complementary sticky-end sequences with bridging strands attached to hypothetical origami-Y. These interactions will prevent origami-Y from interacting with origami-X, leaving origami-Y in its monomeric form. This model cannot explain the presence of 0.4%–1.4% monomers in gel-purified samples (Figure 5), however, as excess bridging strands were not present. We have previously measured the heterodimerization reaction rate of origami systems similar to the one studied here using single-molecule fluorescence and found it to be 1.87×10^6 M^{-1} s^{-1} (measured at 10×10^{-3} M Mg^{+2} with monomers purified using size-exclusion chromatography).[42] In the absence of interfering mechanisms, this reaction rate should allow essentially complete heterodimerization within the 48-h reaction time used in the current study (>99.9% yield, see Experimental Section). Our previous analysis also suggests that heterodimers should not dissociate under the conditions used in the current study. Therefore, a thermodynamic equilibrium cannot explain the presence of unreacted monomers observed here. In principle, origami structural defects may also contribute to the presence of unreactive monomers. However, origami structures with a visible structural defect in the BSE site (≈1%–2% of the monomers) were not considered in the analysis (see Experimental Section), and structural defects that were too small to be visualized by the AFM (e.g., the absence of some bridging strands) are unlikely significant enough to prevent formation of a stable heterodimer.[42] In addition, it is possible that origami monomers adhere to the Eppendorf tube surface hindering heterodimerization, and resulting in the small percentage of monomers in both gel- and PEG-purified samples.

Formation of FFG and FGG heterotrimers: We also observed FFG and FGG heterotrimers in the PEG-purified samples. One possibility is that unpurified stable FF and GG homodimers of the BSE–PTE type interact through the unbound BSEs (rightmost edge of FF homodimers or leftmost edge of GG homodimers, respectively) with the additional origami-G or origami-F, forming the observed FFG or FGG heterotrimers, respectively (Figure 5b). Another possibility is that free bridging strands that remain in solution after PEG precipitation replace native poly-T loop strands belonging to the other origami type through a toehold-mediated strand displacement reaction (a reaction that is kinetically and thermodynamically possible due to origami-F and origami-G homology and the likely availability of scaffold toehold, see further discussion in Figure S12, Supporting Information). This would change the addressability of the origami monomer allowing interaction with additional native origami of the same type and the formation of the observed heterotrimers. These models are both supported by the fact the heterotrimers were not observed in the gel-purified samples. However, lack of clear dependency of the level of heterotrimers on the number of PEG purifications performed (Figure 5a) and on the design of the BSEs prevents us from determining to what degree each of these two mechanisms are responsible for the presence of heterotrimers.

3.2. Dependence of Heterodimerization Yields on Bridging-Strand Design

Because homodimer formation depends strongly on the number of bridging strands and lengths of the sticky ends (Figure 2a,b), we initially hypothesized that the heterodimerization yields would depend significantly on the BSE design.[42] However, our results showed only weak dependence on this design (Figure 3b). This can be largely explained by the fact that almost all the BSE–BSE homodimers, which were the majority of homodimers, dissociated in the presence of the other origami type, allowing formation of the correct heterodimers (Figure 5). Experimental statistical noise and the existence of alternative models for the formation of the FFG and FGG heterodimers prevent us from determining, at this point, whether the small differences in heterodimerization yields are the results of differences in bridging-strand designs or other factors. For example, 11-nt sticky ends complete a full helical turn and, therefore, are more likely to form blunt-end interactions with the origami helices than are the 8-nt sticky ends. Since both designs have enough dimerization binding energy as we showed before,[42] however, it is not clear whether this presumed interaction explains the somewhat higher yields observed for the gel purified FG23/11 and FG11/11 in comparison to FG23/8 and FG11/8 (Figure 3b).

3.3. The Mechanisms of Origami Non-Specific Interactions

As is shown in Figure 2b, longer sticky ends decrease the formation of homodimers and larger structures, and the AFM images show that for most of the homodimers the two monomers maximize (or come close to maximizing) the number of contacts: The two origami units are shifted minimally or not at all with respect to one another. Therefore, it is likely that these are stacking interactions between the ends of the bridging strands and scaffold helices (typically called blunt-end stacking interactions) and not interactions of sticky-end segments. This conclusion is supported by the fact that the BSE–BSE homodimer interaction sites typically showed minimal or no observable gap between the helices of the two origami units (Figure 4) as would be expected for a blunt-end interaction. To allow blunt-end interactions, the overhanging single-stranded sticky ends must be pushed aside (likely above or under the origami plane). Presuming that longer sticky ends are less likely to be displaced, longer sticky ends are expected to reduce homodimerization, in agreement with our results (Figures 2b). Edge scaffold loops and poly-T loops are each attached to the origami core through two connections and are therefore presumably less likely to be pushed aside than sticky ends that are attached to the origami core through a single connection (see schematics in Figure 1d). Thus, an increased number of bridging strands (at the expense of scaffold loops or poly-T loops) are expected to increase blunt-end interactions, in agreement with our results (Figures 2b). According to this model, BSE–BSE interactions are more likely than BSE–PTE interactions, which in turn, are more likely than PTE–PTE interactions, again in agreement with our results (Figure 4).

Our results show that among the BSE–BSE interactions formed in the annealing process, those involving origami-F were more frequently in the flip orientation and those involving origami-G were more frequently in the rotate orientation (the only possible BSE–BSE interactions, Figure 4, monomers purified by PEG). This orientation preference is maintained for BSE–BSE interactions formed after the annealing process, although with lower frequency differences between orientations (Figure 4, monomers purified by gel). Attempts to identify a straightforward structural rule that determines the preferred BSE–BSE orientation in computer-visualized origami structures modeled by placing two monomer units in the corresponding orientations using Visual Molecular Dynamics software[59] (data not shown), by considering bridging strands and scaffold strands directionality (in terms of 5′→3′, see schematics, Figure 4), or by considering the nucleotides content in the blunt-ends[60] were not fruitful. The preferred orientations of blunt-end interactions between two short DNA helices were studied in silico using all-atom simulations by Aksimentiev and co-workers.[61] Expanding this approach to origami structures may shed light on the origami-edge interaction mechanisms on the atomic level.

4. Conclusions

In this work, we established that proper purification of origami building blocks from excess strands and homodimers and larger structures preformed in the thermal annealing process is essential for achieving high hetero-origami attachment yields. Specifically, purification of rectangle origami building blocks using agarose gel electrophoresis reduced unreactive monomers and incorrect structures by 4- to 25-fold compared to PEG-purified samples, achieving 98.6%–99.6% heterodimerization yields. To the best of our knowledge, these are the highest sticky end-based origami heterodimerization yields achieved thus far. We suggest that unpurified bridging strands from one type of monomer can interact with origami monomers of the other type, blocking the desired interaction with a monomer and considerably reducing heterodimerization yields when these strands are not properly purified. Formation of homodimers (and to lesser extent, larger structures) through blunt-end interactions strongly depend on the design of the origami edges. Designs with higher numbers of bridging strands and shorter sticky ends increased non-specific blunt-end interactions. Importantly, however, the many homodimers formed through the interaction of BSEs dissociated in the presence of the other origami type, and, as a result, the design of the BSEs had only minor effects on heterodimerization yields. This observation is in agreement with a previously proposed model that suggested that the ability to escape kinetic traps is essential for achieving the desired origami attachment in high yields.[53] The mechanisms responsible for the interaction of BSEs with poly-T-loop edge of the same origami type, resulting in formation of heterotrimers, are not entirely clear. Changing the poly-T-loop edge design, for example, such that formation of toehold and the subsequent poly-T displacement would be less likely, may allow the question to be addressed, and we intend to test this in the future. More generally, this work demonstrates that competing, unwanted side reactions—rather than thermodynamic

instability—are the major factors that limit our ability to fabricate complex DNA structures with high yield. We reached a similar conclusion regarding the performance of DNA bipedal motors.[24] These results indicate that more attention should be paid to potentially interfering side reactions. Finally, the significant reduction in incorrect interactions and structures achieved in this work by implementing gel purification of the origami building blocks should allow sticky-end-based fabrication of structures made of multiple different origami building blocks.

5. Experimental Section

Origami Design and Assembly: The origami monomers were designed based on Rothemund rectangle origami[1] with minor modifications (for strand sequences, see, Table S1, Supporting Information). Staples, poly-T loops, and bridging strands (purchased from IDT) were used unpurified, and the scaffold was M13mp18 (Type p7249, Tilibit Nanosystems). The base compositions of the sticky ends were generated randomly but such that the GC content for each sequence was about 50%. NUPACK[62] analysis of the sticky-end sequences showed that none of the sequences self- or cross-hybridized at more than 0.1%[42] (for strand sequences, see Table S1, Supporting Information). Assembly was performed separately for origami-F and origami-G in 1 × TAE buffer (40×10^{-3} M Tris, 1×10^{-3} M EDTA, 20×10^{-3} M acetic acid, pH 8.0) containing 12×10^{-3} M $MgCl_2$ in a 50 µL volume. Thermal annealing procedure was as follows: samples were heated at 65 °C for 15 min, cooled to 40 °C at 1 °C/15 min, and cooled to 20 °C at 1 °C/10 min using a thermal cycler (Esco, SwiftMaxPro). The solution contained 20×10^{-9} M scaffold, fivefold excess staples, and 12- or 5-fold excess T-loops and bridging strands.

PEG Purification: After annealing, monomers were purified from excess staples using PEG as a precipitating agent. Typically, 1 × TE buffer (10×10^{-3} M Tris, pH 8.0, 1×10^{-3} M EDTA) containing 15% (w/v) PEG-8000 and 500×10^{-3} M NaCl was added to the origami sample at equal volume in an Eppendorf tube and mixed gently. The mixture was centrifuged at 17 800 × g for 30 min at 4 °C. The supernatant was withdrawn carefully, and the pellet was re-suspended in 1 x TAE buffer supplemented with 4×10^{-3} M $MgAc_2$. This purification procedure was either carried out once or twice (Figure 3c). In addition, this procedure is also used to increase the concentration of monomers after extraction from gels.

Gel Purification: For gel purification of origami monomers, the origami samples were loaded into wells of a 1% agarose gel prepared from SeaKem LE agarose with 1 × TAE buffer containing 1 x SYBR Safe stain (Invitrogen), supplemented with 4 or 12×10^{-3} M $MgCl_2$ or 100×10^{-3} M NaCl. The running buffer was 1 x TAE with the identical salt. Gels that were prepared with TBE buffers yielded similar chromatograms to those prepared with TAE, and because it is easier to handle TAE subsequent experiments used this buffer. The gel (10-cm length) was run for 1.5–2 h in an ice-cold water bath at 80 V for magnesium-containing buffers or 50 V for NaCl-containing buffers. Origami monomers were extracted from the NaCl gel using Freeze 'N Squeeze Quantum Prep columns (BioRad). The monomer bands of interest were cut from the gel, chopped with a razor, placed in the column and placed at −20 °C for 10 min. The samples were spun at 13 000 × g for 5 min at 4 °C. The samples were then transferred from the collection tubes to 1.5-mL Eppendorf tubes. To increase the monomer concentration to about 2×10^{-9} M after gel purification, the same PEG precipitation procedure was used as described above.

Heterodimerization Reaction: Origami-F and origami-G monomers were brought to equal concentrations of about 10×10^{-9} M after PEG purification or 2×10^{-9} M after gel purification, as determined using a Nanodrop spectrophotometer (ThermoFisher Scientific). Equal volumes of the two monomers (10 µL) were gently stirred in a shaker (150 rpm) at room temperature for 1 h, then the $MgAc_2$ concentration was titrated to 12×10^{-3} M using 32×10^{-3} M $MgAc_2$ in 1 x TAE solution over 6 h. The total heterodimerization reaction time was 48 h. Based on the heterodimerization rates previously measured by us[42] and because it was almost impossible to make the concentrations of the two monomers identical, this reaction time should be sufficient to allow at least 99.9% heterodimerization yields when the initial monomer concentration is 2×10^{-9} M. It was chosen to work at 10 and 2×10^{-9} M of PEG and gel purified monomers, respectively, because these concentrations were best fit to the amount of purified monomers recovered from the PEG and gel procedures and sample volumes required for the heterodimerization reaction.

AFM Imaging: For liquid-AFM imaging on a Cypher (Asylum Research), 5–7 µL of the sample (12×10^{-3} M Mg^{2+} concentration) was deposited onto freshly cleaved mica and left to adsorb for 5 min. The measurement was conducted under this liquid buffer and on an active antivibration table in liquid tapping mode using a HiRES-C14/AlBS probe (MikroMasch) at a scan rate of 3 min per $2 \times 2 \times 10^{-6}$ M image size. For high-resolution imaging of the dimer attachment sites, scanning was performed at about 3 min per $0.2 \times 0.2 \times 10^{-6}$ M image size.

Identification of Origami Type and Orientation and Determination of Heterodimerization Yields: The origami type and orientation in the dimers and trimers were visually determined by two independent researchers with 98%–99% consensus typically achieved. Disagreements were resolved either by mutual reanalysis or by averaging the data from the two researchers, and the results were considered as a one-data point. Origami structures that were visibly broken in the BSE sites (≈1%–2%, likely because of the AFM tip) or origami with unreadable letters were not considered in the analysis. Only dimers with the correct FG orientation were considered as heterodimers for the calculation of heterodimerization yields. Achieving equimolar concentrations of origami-F and origami-G was almost impossible, and therefore one of the two units was always observed more frequently in the AFM images than the other. For this reason, heterodimerization yields were defined as the number of correctly formed heterodimers divided by the number of the less frequent monomer type. Experiments were repeated at least three times for each data point, and the total number of origami monomers in each of these experiments was 300–1000 (larger numbers of origami units for in the high-yield cases). The error bars in the measurements of heterodimerization yields are the standard deviations calculated from these three or more independent experiments.

Supporting Information

Supporting Information is available from the Wiley Online Library or from the author.

Acknowledgements

B.S. and M.L. contributed equally to this work. This work was supported by grant from the Israel Science Foundation (1857/17). M.L. was supported by the Darom Fellowship, and Y.B. was supported by the Negev Fellowship.

Conflict of Interest

The authors declare no conflict of interest.

Keywords

agarose gel electrophoresis, DNA molecular devices, DNA nanotechnology, DNA origami

Received: June 7, 2019
Revised: September 30, 2019
Published online:

[1] P. W. Rothemund, *Nature* **2006**, *440*, 297.
[2] N. C. Seeman, O. Gang, *MRS Bull.* **2017**, *42*, 904.
[3] N. Liu, T. Liedl, *Chem. Rev.* **2018**, *118*, 3032.
[4] M. R. Jones, N. C. Seeman, C. A. Mirkin, *Science* **2015**, *347*, 1260901.
[5] F. Hong, F. Zhang, Y. Liu, H. Yan, *Chem. Rev.* **2017**, *117*, 12584.
[6] W. Pfeifer, B. Sacca, *ChemBioChem* **2016**, *17*, 1063.
[7] M. Pilo-Pais, S. Goldberg, E. Samano, T. H. Labean, G. Finkelstein, *Nano Lett.* **2011**, *11*, 3489.
[8] S. Pal, Z. Deng, H. Wang, S. Zou, Y. Liu, H. Yan, *J. Am. Chem. Soc.* **2011**, *133*, 17606.
[9] B. Ding, Z. Deng, H. Yan, S. Cabrini, R. N. Zuckermann, J. Bokor, *J. Am. Chem. Soc.* **2010**, *132*, 3248.
[10] H. Bui, C. Onodera, C. Kidwell, Y. Tan, E. Graugnard, W. Kuang, J. Lee, W. B. Knowlton, B. Yurke, W. L. Hughes, *Nano Lett.* **2010**, *10*, 3367.
[11] S. Pal, Z. Deng, B. Ding, H. Yan, Y. Liu, *Angew. Chem., Int. Ed.* **2010**, *49*, 2700.
[12] R. Schreiber, J. Do, E. M. Roller, T. Zhang, V. J. Schuller, P. C. Nickels, J. Feldmann, T. Liedl, *Nat. Nanotechnol.* **2014**, *9*, 74.
[13] Z. Zhao, J. Fu, S. Dhakal, A. Johnson-Buck, M. Liu, T. Zhang, N. W. Woodbury, Y. Liu, N. G. Walter, H. Yan, *Nat. Commun.* **2016**, *7*, 10619.
[14] B. Sacca, R. Meyer, M. Erkelenz, K. Kiko, A. Arndt, H. Schroeder, K. S. Rabe, C. M. Niemeyer, *Angew. Chem., Int. Ed.* **2010**, *49*, 9378.
[15] K. Numajiri, M. Kimura, A. Kuzuya, M. Komiyama, *Chem. Commun.* **2010**, *46*, 5127.
[16] N. V. Voigt, T. Torring, A. Rotaru, M. F. Jacobsen, J. B. Ravnsbaek, R. Subramani, W. Mamdouh, J. Kjems, A. Mokhir, F. Besenbacher, K. V. Gothelf, *Nat. Nanotechnol.* **2010**, *5*, 200.
[17] H. T. Maune, S. P. Han, R. D. Barish, M. Bockrath, W. A. Goddard III, P. W. Rothemund, E. Winfree, *Nat. Nanotechnol.* **2010**, *5*, 61.
[18] A. P. Eskelinen, A. Kuzyk, T. K. Kaltiaisenaho, M. Y. Timmermans, A. G. Nasibulin, E. I. Kauppinen, P. Torma, *Small* **2011**, *7*, 746.
[19] J. Zessin, F. Fischer, A. Heerwig, A. Kick, S. Boye, M. Stamm, A. Kiriy, M. Mertig, *Nano Lett.* **2017**, *17*, 5163.
[20] H. Gu, J. Chao, S. J. Xiao, N. C. Seeman, *Nature* **2010**, *465*, 202.
[21] S. F. Wickham, M. Endo, Y. Katsuda, K. Hidaka, J. Bath, H. Sugiyama, A. J. Turberfield, *Nat. Nanotechnol.* **2011**, *6*, 166.
[22] S. F. Wickham, J. Bath, Y. Katsuda, M. Endo, K. Hidaka, H. Sugiyama, A. J. Turberfield, *Nat. Nanotechnol.* **2012**, *7*, 169.
[23] T. E. Tomov, R. Tsukanov, M. Liber, R. Masoud, N. Plavner, E. Nir, *J. Am. Chem. Soc.* **2013**, *135*, 11935.
[24] T. E. Tomov, R. Tsukanov, Y. Glick, Y. Berger, M. Liber, D. Avrahami, D. Gerber, E. Nir, *ACS Nano* **2017**, *11*, 4002.
[25] E. Kopperger, J. List, S. Madhira, F. Rothfischer, D. C. Lamb, F. C. Simmel, *Science* **2018**, *359*, 296.
[26] J. J. Funke, P. Ketterer, C. Lieleg, S. Schunter, P. Korber, H. Dietz, *Sci. Adv.* **2016**, *2*, e1600974.
[27] P. C. Nickels, B. Wunsch, P. Holzmeister, W. Bae, L. M. Kneer, D. Grohmann, P. Tinnefeld, T. Liedl, *Science* **2016**, *354*, 305.
[28] S. M. Douglas, I. Bachelet, G. M. Church, *Science* **2012**, *335*, 831.
[29] A. J. Thubagere, W. Li, R. F. Johnson, Z. Chen, S. Doroudi, Y. L. Lee, G. Izatt, S. Wittman, N. Srinivas, D. Woods, E. Winfree, L. Qian, *Science* **2017**, *357*, eaan6558.
[30] M. Endo, Y. Katsuda, K. Hidaka, H. Sugiyama, *Angew. Chem., Int. Ed.* **2010**, *49*, 9412.
[31] A. N. Marchi, I. Saaem, B. N. Vogen, S. Brown, T. H. LaBean, *Nano Lett.* **2014**, *14*, 5740.
[32] W. Liu, H. Zhong, R. Wang, N. C. Seeman, *Angew. Chem., Int. Ed.* **2011**, *50*, 264.
[33] R. Jungmann, M. Scheible, A. Kuzyk, G. Pardatscher, C. E. Castro, F. C. Simmel, *Nanotechnology* **2011**, *22*, 275301.
[34] Z. Li, L. Wang, H. Yan, Y. Liu, *Langmuir* **2012**, *28*, 1959.
[35] Z. Li, M. Liu, L. Wang, J. Nangreave, H. Yan, Y. Liu, *J. Am. Chem. Soc.* **2010**, *132*, 13545.
[36] K. F. Wagenbauer, C. Sigl, H. Dietz, *Nature* **2017**, *552*, 78.
[37] S. M. Douglas, H. Dietz, T. Liedl, B. Hogberg, F. Graf, W. M. Shih, *Nature* **2009**, *459*, 414.
[38] R. Schreiber, S. Kempter, S. Holler, V. Schuller, D. Schiffels, S. S. Simmel, P. C. Nickels, T. Liedl, *Small* **2011**, *7*, 1795.
[39] J. Fern, J. Lu, R. Schulman, *ACS Nano* **2016**, *10*, 1836.
[40] J. Zenk, C. Tuntivate, R. Schulman, *J. Am. Chem. Soc.* **2016**, *138*, 3346.
[41] M. Liber, T. E. Tomov, R. Tsukanov, Y. Berger, E. Nir, *Small* **2015**, *11*, 568.
[42] M. Liber, T. E. Tomov, R. Tsukanov, Y. Berger, M. Popov, D. C. Khara, E. Nir, *Small* **2018**, *14*, 1800218.
[43] T. C. Wu, M. Rahman, M. L. Norton, *Acc. Chem. Res.* **2014**, *47*, 1750.
[44] R. Wang, K. Gorday, C. Nuckolls, S. J. Wind, *Chem. Commun.* **2016**, *52*, 1610.
[45] S. Woo, P. W. Rothemund, *Nat. Chem.* **2011**, *3*, 620.
[46] T. Gerling, K. F. Wagenbauer, A. M. Neuner, H. Dietz, *Science* **2015**, *347*, 1446.
[47] P. Ketterer, E. M. Willner, H. Dietz, *Sci. Adv.* **2016**, *2*, e1501209.
[48] J. Ye, S. Helmi, J. Teske, R. Seidel, *Nano Lett.* **2019**, *19*, 2707.
[49] A. Rajendran, M. Endo, Y. Katsuda, K. Hidaka, H. Sugiyama, *ACS Nano* **2011**, *5*, 665.
[50] M. Endo, T. Sugita, Y. Katsuda, K. Hidaka, H. Sugiyama, *Chem.—Eur. J.* **2010**, *16*, 5362.
[51] M. Endo, T. Sugita, A. Rajendran, Y. Katsuda, T. Emura, K. Hidaka, H. Sugiyama, *Chem. Commun.* **2011**, *47*, 3213.
[52] G. Tikhomirov, P. Petersen, L. Qian, *Nat. Nanotechnol.* **2017**, *12*, 251.
[53] G. Tikhomirov, P. Petersen, L. Qian, *Nature* **2017**, *552*, 67.
[54] Z. Zhao, Y. Liu, H. Yan, *Nano Lett.* **2011**, *11*, 2997.
[55] K. N. Kim, K. Sarveswaran, L. Mark, M. Lieberman, *Soft Matter* **2011**, *7*, 4636.
[56] A. Shaw, E. Benson, B. Hogberg, *ACS Nano* **2015**, *9*, 4968.
[57] E. Stahl, T. G. Martin, F. Praetorius, H. Dietz, *Angew. Chem., Int. Ed.* **2014**, *53*, 12735.
[58] J. Lipfert, S. Doniach, R. Das, D. Herschlag, *Annu. Rev. Biochem.*, **2014**, *83*, 813.
[59] W. Humphrey, A. Dalke, K. Schulten, *J. Mol. Graphics* **1996**, *14*, 33.
[60] F. Kilchherr, C. Wachauf, B. Pelz, M. Rief, M. Zacharias, H. Dietz, *Science* **2016**, *353*, aaf5508.
[61] C. Maffeo, B. Luan, A. Aksimentiev, *Nucleic Acids Res.* **2012**, *40*, 3812.
[62] R. M. Dirks, J. S. Bois, J. M. Schaeffer, E. Winfree, N. A. Pierce, *SIAM Rev.* **2007**, *49*, 65.

